



Published in final edited form as:

Nat Neurosci. 2013 September ; 16(9): 1291–1298. doi:10.1038/nn.3480.

Substrate-selective COX-2 inhibition decreases anxiety via endocannabinoid activation

Daniel J. Hermanson¹, Nolan D. Hartley², Joyonna Gamble-George², Naoko Brown³, Brian C. Shonesy⁴, Phillip J. Kingsley¹, Roger J. Colbran⁴, Jeffrey Reese³, Lawrence J. Marnett¹, and Sachin Patel^{2,4}

Lawrence J. Marnett: larry.marnett@vanderbilt.edu; Sachin Patel: Sachin.patel@vanderbilt.edu

¹A.B. Hancock Jr. Memorial Laboratory for Cancer Research, Departments of Biochemistry, Chemistry, and Pharmacology, Vanderbilt Institute of Chemical Biology, Center in Molecular Toxicology, and Vanderbilt-Ingram Cancer Center

²Departments of Psychiatry Vanderbilt University School of Medicine, Nashville, TN 37232 U.S.A

³Departments of Psychiatry Pediatrics Vanderbilt University School of Medicine, Nashville, TN 37232 U.S.A

⁴Departments of Psychiatry Molecular Physiology and Biophysics, Vanderbilt University School of Medicine, Nashville, TN 37232 U.S.A

Abstract

Augmentation of endogenous cannabinoid (eCB) signaling represents an emerging approach to the treatment of affective disorders. Cyclooxygenase-2 (COX-2) oxygenates arachidonic acid to form prostaglandins, but also inactivates eCBs *in vitro*. However, the viability of COX-2 as a therapeutic target for *in vivo* eCB augmentation has not been explored. Here we utilized medicinal chemistry and *in vivo* analytical and behavioral pharmacological approaches to demonstrate a key role for COX-2 in the regulation of endocannabinoid (eCB) levels *in vivo*. A novel pharmacological strategy involving “substrate-selective” inhibition of COX-2 was used to augment eCB signaling without affecting related non-eCB lipids or prostaglandin synthesis. Behaviorally, substrate-selective inhibition of COX-2 reduced anxiety-like behaviors in mice via increased eCB signaling. These data elucidate a key role for COX-2 in the regulation of eCB signaling and suggest substrate-selective pharmacology represents a viable approach for eCB augmentation with broad therapeutic potential.

Endogenous cannabinoids (eCBs) including anandamide (AEA) and 2-arachidonoylglycerol (2-AG) are lipid-derived signaling molecules that activate the cannabinoid receptors, CB₁

Users may view, print, copy, download and text and data- mine the content in such documents, for the purposes of academic research, subject always to the full Conditions of use: http://www.nature.com/authors/editorial_policies/license.html#terms

Correspondence to: Lawrence J. Marnett, larry.marnett@vanderbilt.edu; Sachin Patel, Sachin.patel@vanderbilt.edu.

Publisher's Disclaimer: Conflict of interest disclaimer: The authors declare a pending patent application for SSCIs including LM-4131.

Supplementary information: Supplementary figures and methods can be found online at www.nature.com/nn.

*LM-4131 is also known as BML-190

and CB₂¹⁻³. eCBs have been implicated in many physiological and pathological processes including metabolic regulation^{4,5}, pain modulation^{6,7}, cognitive and memory function⁸, stress and anxiety modulation^{9,10}, as well as immunological processes such as inflammation^{11,12}, tumor progression^{13,14}, and bone remodeling¹⁵. Augmentation of eCB signaling via inhibition of the eCB degrading enzymes fatty acid amide hydrolase (FAAH), which regulates AEA levels¹⁶, and monoacylglycerol lipase (MAGL), which regulates 2-AG levels¹⁷, has demonstrated preclinical efficacy in a variety of pathological processes including mood and anxiety disorders^{10,18-23}. However, both strategies lack selectivity for modulating eCB lipids over structurally related non-eCB lipids. Elucidation of novel molecular targets and pharmacological approaches to augment eCB signaling with higher selectivity could have broad therapeutic implications²⁴⁻²⁶.

Cyclooxygenase-2 (COX-2) catalyzes the formation of prostaglandins (PGs) from arachidonic acid (AA) and is the pharmacological target of non-steroidal antiinflammatory drugs (NSAIDs). COX-2 also efficiently oxygenates and inactivates 2-AG, to produce prostaglandin-glycerol esters (PG-Gs), and AEA, to produce prostaglandin ethanolamides (PG-EAs)^{27,28}. COX-2 inhibition enhances eCB-mediated retrograde synaptic suppression and extends the stability of exogenously administered AEA^{29,30}. Moreover, some of the antinociceptive effects of COX-2 inhibitors are mediated via cannabinoid receptors, suggesting activation of eCB signaling by COX-2 inhibition^{31,32}. Although these data suggest a role for COX-2 in the regulation of eCB signaling, direct evidence for the *in vivo* regulation of eCBs by COX-2 is lacking, as is a viable pharmacological strategy to modulate eCB levels via COX-2 inhibition without also profoundly affecting PG synthesis.

We recently reported that rapid-reversible inhibitors of COX-2 selectively inhibit the oxygenation of 2-AG and AEA with much lower IC₅₀'s than for AA, a phenomenon we termed “substrate-selective” inhibition of COX-2^{33,34}. Despite these initial studies, neither the molecular basis for substrate-selective inhibition, nor the *in vivo* efficacy of substrate-selective COX-2 inhibitors (SSCIs) to augment eCB signaling has been demonstrated. Here we elucidate the molecular determinants of substrate-selective pharmacology *in vitro* and develop the first *in vivo* biologically active SSCI with anxiolytic effects in preclinical models.

Results

Development of *in vivo* bioactive SSCIs

To develop novel *in vivo* biologically active SSCIs, we utilized site-directed mutagenesis of COX-2 active site residues to identify the key molecular interactions required for SSCI. Previous studies have established that mutations of Arg-120 and Tyr-355 of COX-2 drastically reduce the ability of the COX inhibitor indomethacin to inhibit AA oxygenation by eliminating its ability to ion-pair and hydrogen bond with COX-2³⁶. However, we found that indomethacin still potently inhibits eCB oxygenation by the COX-2 R120Q and Y355F mutants (Fig. 1 a-d). This indicates that, although ion-pairing and hydrogen-bonding with Arg-120 and Tyr-355 are critical for indomethacin inhibition of AA oxidation to PGs, they are much less important for inhibition of eCB oxygenation.

Therefore we synthesized and screened a small library of tertiary amide derivatives of indomethacin, which have a reduced capacity to ion-pair and hydrogen bond with Arg-120 and Tyr-355. Each of the tertiary amides inhibited eCB oxygenation by COX-2 but did not inhibit AA oxygenation (Supplemental Fig. 1). The morpholino amide of indomethacin, LM-4131* (Fig. 1e), was effective at inhibiting eCB oxygenation by purified COX-2 and by COX-2 in lipopolysaccharide-activated RAW 264.7 macrophages without inhibiting AA oxygenation (Fig. 1 f-g). Moreover, LM-4131 concentration-dependently increased 2-AG levels in stimulated RAW 264.7 macrophages without increasing AA levels, providing cellular evidence for substrate-selective pharmacology of LM-4131 (Fig. 1 h). Importantly, LM-4131 did not inhibit other eCB metabolizing/synthetic enzymes including FAAH, MAGL, or DAGL α (Fig. 1 i-k). Thus, LM-4131 exhibits multiple properties desirable in a SSCI, and was selected for subsequent *in vivo* studies.

***In vivo* augmentation of eCB levels by LM-4131 via SSCI**

To assess the ability of LM-4131 to modulate eCB levels *in vivo*, we administered LM-4131 to male ICR mice via intraperitoneal (i.p.) injection and analyzed levels of eCBs, PGs, and AA two hours after administration. We found that LM-4131 significantly increased whole brain AEA levels at 3 mg/kg ($p < 0.01$) and 10 mg/kg ($p < 0.0001$) with a non-significant trend to increase 2-AG levels at the highest dose (Fig. 2 a-b). LM-4131 did not affect AA levels or PG levels at any dose tested (Fig. 2 c-d), demonstrating that the substrate-selectivity of LM-4131 is retained *in vivo*. To quantify the magnitude of the increase in brain eCBs induced by LM-4131 treatment, we conducted a meta-analysis of data obtained from 12 cohorts of animals, normalizing eCB levels in each animal to mean eCB levels in the respective vehicle control group. This analysis revealed that, on average, LM-4131 at 10 mg/kg significantly increased AEA to 139% of vehicle ($p < 0.0001$), and increased 2-AG levels to 109% of vehicle ($p < 0.01$; Fig. 2 e-f). Analysis of brain extracts by LC-MS/MS revealed the presence of LM-4131, but not indomethacin, after LM-4131 treatment (Supplemental Fig. 1). Thus, LM-4131 selectively increases eCB levels without affecting AA or PG levels, and is present in the brain 2 hours after i.p. injection.

To confirm that the *in vivo* substrate-selective profile of LM-4131 is unique relative to other COX inhibitors, we determined the ability of indomethacin (10 mg/kg), a non-selective COX-1/COX-2 inhibitor and the parent compound of LM-4131, the COX-2 selective inhibitor NS-398 (10 mg/kg), and the COX-1 selective inhibitor SC-560 (10 mg/kg), to modulate eCB, AA, and PG levels *in vivo*. LM-4131 ($p < 0.0001$), indomethacin ($p < 0.0001$), NS-398 ($p < 0.001$) and SC-560 ($p < 0.01$) significantly increased AEA levels, while only LM-4131 ($p < 0.01$) and indomethacin ($p < 0.01$) significantly increased 2-AG levels (Fig. 2 g-h). LM-4131 did not significantly affect AA levels, while indomethacin ($p < 0.001$), NS-398 ($p < 0.01$), and SC-560 ($p < 0.01$) all significantly increased AA levels (Fig. 2 i). Indomethacin, NS-398, and SC-560 ($p < 0.0001$ for all), but not LM-4131, profoundly

Author contributions: LM-4131 was synthesized and characterized *in vitro* by DJH in the laboratory of LJM. *In vivo* biochemical and behavioral experiments were designed, executed, and analyzed by DJH, NDH, and SP in the laboratory of SP. Analysis of LM-4131 hydrolysis was performed by DJH and PJK in the laboratory of LJM. Analysis of LM-4131 inhibition of MAGL and DAGL was performed by DJH and BCS in the laboratory of RJC. JG-G completed cannabinoid tetrad behavioral studies in the laboratory of SP. *Ptgs2*^{-/-} mice were bred and genotyped by NB in the laboratory of JR. The manuscript was written by DJH, LM and SP, and edited by all authors. LJM and SP take responsibility for the accuracy of the data and were in full control of all data presented

decreased brain PG levels (Fig. 2 j). These data indicate that the *in vivo* substrate-selective pharmacological profile of LM-4131 is unique, and not shared by traditional COX inhibitors.

We next confirmed COX-2 as the *in vivo* molecular target mediating the increase in brain eCBs observed after LM-4131 treatment using COX-2 knock-out (*Ptgs2*^{-/-}) mice. LM-4131 (10 mg/kg) significantly increased AEA (p<0.01) and 2-AG (p<0.05) levels in WT, but not *Ptgs2*^{-/-} littermates (Fig. 2 k-l). Importantly, *Ptgs2*^{-/-} mice had significantly higher brain AEA levels than WT littermates at baseline (p<0.0001). Lastly, LM-4131 did not affect AA or PG levels in WT or *Ptgs2*^{-/-} mice (Fig. 2 m-n). These data confirm that LM-4131 increases brain eCB levels via a COX-2 dependent mechanism, and COX-2 substantially regulates basal brain AEA levels *in vivo*.

LM-4131 selectively increases eCBs over structurally related non-eCB lipids

One major limitation of currently available eCB degradation inhibitors is their lack of selectivity for eCBs over related non-eCB lipids. FAAH inhibition increases AEA levels, but also increases levels of N-acylethanolamides (NAEs; oleoylethanolamide (OEA), palmitoylethanolamide (PEA), and stearoylethanolamide (SEA)). Similarly MAGL inhibition increases 2-AG levels, but also related monoacylglycerols (MAGs) including 2-oleoylglycerol (2-OG), 2-palmitoylglycerol (2-PG), and 2-stearoylglycerol (2-SG). Given the selectivity of COX-2 for AA-containing lipids, we hypothesized that LM-4131 would be selective for increasing AEA and 2-AG over other NAEs and MAGs. To test this hypothesis, we conducted targeted lipid profiling of NAEs and MAGs after LM-4131 treatment. As expected, LM-4131 significantly increased brain AEA (p< 0.0001; Fig. 3 a), but not any other NAE. In contrast, the FAAH inhibitor PF-3845^{37,38} (10 mg/kg) robustly increased all NAEs including AEA (Fig. 3b). These data strongly suggest that LM-4131 selectively increases brain AEA over other NAEs, and that its mechanism of action is not via off target FAAH inhibition, since if this were the case we would expect to see increases in other NAEs also.

To further exclude FAAH inhibition as contributing to the AEA elevating effects of LM-4131 we conducted several additional experiments. First, we found that LM-4131 caused a significant additional increase in AEA levels (p<0.01) when combined with the FAAH inhibitor PF-3845, compared to PF-3845 treatment alone (Fig. 3c), suggesting different mechanisms of action. Second, we found that LM-4131 did not affect levels of any NAE in the liver, which has very high FAAH expression, while PF-3845 caused robust increases in levels of all NAEs (Fig. 3 d). Lastly, we found that LM-4131 increased brain AEA levels in WT and *Faah*^{-/-} mice to a similar extent (Fig. 3 e). Taken together with our biochemical data that LM-4131 does not inhibit FAAH activity *in vitro*, these converging *in vivo* data strongly suggest a unique COX-2 mediated mechanism of action of LM-4131 to increase AEA levels.

We also tested the selectivity of LM-4131 for 2-AG over other MAGs compared to the MAGL inhibitor JZL-184 (40 mg/kg). While LM-4131 (10 mg/kg) significantly increased brain 2-AG levels (p<0.05), it did not affect levels of any other MAG (Fig. 3 f). In contrast, the MAGL inhibitor JZL-184 increased levels of 2-AG and 3 other MAG species (Fig. 3 g).

Furthermore, LM-4131 produced an additional significant increase in 2-AG levels after JZL-184 treatment ($p < 0.05$) compared to JZL-184 alone (Fig. 3 h). Combined with our *in vitro* data that LM-4131 does not affect MAGL activity, these *in vivo* data strongly suggest that the ability of LM-4131 to increase 2-AG levels is not mediated via MAGL inhibition.

Lastly, we wanted to determine the selectivity of the regulation of basal brain eCBs by COX-2 over related non-eCB NAEs. We therefore determined the effect of LM-4131 on brain NAEs in WT and *Ptgs2*^{-/-} mice. We again found that LM-4131 significantly increased brain AEA ($p < 0.001$), but no other NAE (Fig. 3 h), and importantly, *Ptgs2*^{-/-} mice had increased levels of only AEA ($p < 0.001$), but no other NAE. These data confirm a key role for COX-2 in the selective regulation of basal AEA over other non-eCB NAEs.

LM-4131 increases peripheral eCB levels

Like other eCB degrading enzymes including FAAH and MAGL, COX-2 is expressed in many tissues. We therefore tested the effect of LM-4131 on eCB, NAE, MAG, and PG levels in a variety of peripheral tissues. LM-4131 (10 mg/kg) significantly increased AEA levels in the stomach ($p < 0.05$), small intestine ($p < 0.05$), kidney ($p < 0.0001$), and lung ($p < 0.001$) but not heart (Fig. 4 a-e) or liver (see Fig. 3 d). In contrast, LM-4131 did not affect levels of any other NAE in any tissue. Similarly, LM-4131 had no effect on 2-AG or any other MAG in any peripheral tissue examined (Fig. 4 a-e). To confirm that LM-4131 retained substrate-selective pharmacology outside the CNS, we measured levels of PGs in each tissue after LM-4131 and indomethacin treatment. As expected, indomethacin robustly decreased PGs in all tissues examined ($p < 0.0001$ for stomach, heart, kidney and lung; $p < 0.001$ for intestine), while LM-4131 had no effect on PG levels in any tissue examined (Fig. 4 a-e). These data indicate that SSCI can selectively augment AEA levels without affecting non-eCB NAEs in peripheral tissues, and that LM-4131 retains *in vivo* substrate-selectivity in peripheral tissues.

LM-4131 reduces anxiety via eCB augmentation

Since eCB augmentation via FAAH inhibition has been suggested to represent a novel approach to the treatment of mood and anxiety disorders^{22,26}, in a proof-of-concept study, we assessed the behavioral effects of LM-4131 in pre-clinical models of anxiety. Previous work has shown that FAAH inhibitors are anxiolytic in the novel open-field arena³⁹, and in agreement with this we found that the FAAH inhibitor PF-3845 (10 mg/kg) increased center distance travelled and center time in the open-field arena (Fig. 5 a). Importantly, LM-4131 (10 mg/kg) also increased center distance traveled and center time (Fig. 5b), suggesting it has similar behavioral effects to a FAAH inhibitor with respect to reducing anxiety in this assay. To test the hypothesis that all COX inhibitors that increase brain AEA exert a similar behavioral profile to LM-4131, we tested the effect of indomethacin (10 mg/kg), NS-398 (10 mg/kg), and SC-560 (10 mg/kg) in the open-field arena (Supplemental Fig. 2 a-b). Indomethacin and NS-398, which both increased brain AEA levels, increased center time and center distance traveled in the open-field arena suggestive of an anxiolytic behavioral effect. However, SC-560, which had only marginal effects on brain AEA levels, did not have any significant behavioral effect in this assay (Supplemental Fig. 2 c).

To determine if the behavioral effects of LM-4131 were mediated by substrate-selective inhibition of COX-2, we tested the behavioral effects of LM-4131 in *Ptgs2*^{-/-} mice and WT littermates. While exhibiting a normal anxiolytic-like response in WT littermates (Fig. 5 c-e), LM-4131 did not produce any significant behavioral effects in *Ptgs2*^{-/-} mice (Fig. 5 c-e), in accordance with the lack of change in AEA levels seen after LM-4131 administration to *Ptgs2*^{-/-} mice. Interestingly, *Ptgs2*^{-/-} mice showed a slight anxiolytic phenotype relative to WT littermates on center time spent in the open field (Supplemental Fig. 3), however the exact mechanisms subserving this effect remain unknown.

Since the anxiolytic effects of FAAH inhibition are mediated via AEA acting on CB₁ cannabinoid receptors^{22,40}, we next tested the role of CB₁ receptors in the anxiolytic-like behavioral effects of LM-4131 in the open field arena. While again exerting anxiolytic actions in vehicle-pretreated mice, LM-4131 had no significant behavioral effect in mice treated with the CB₁ receptor antagonist Rimonabant at 3 mg/kg (Fig. 5 f-h). Furthermore, LM-4131 did not produce any behavioral effect in CB₁ receptor knock-out mice (*Cnr1*^{-/-}; Supplemental Fig. 4 a). To verify that LM-4131 actually increased eCB levels in *Cnr1*^{-/-} mice, we analyzed the eCB levels and PG levels in *Cnr1*^{-/-} mice after LM-4131 treatment and found that LM-4131 increased AEA and 2-AG levels in the brains of the *Cnr1*^{-/-} mice while again having no effect on PG levels (Supplemental Fig. 4 b). These data suggest that the behavioral effects of LM-4131 are mediated via substrate-selective inhibition of COX-2, which selectively increases brain eCB levels leading to increased activation of central CB₁ receptors and anxiolytic behavioral effects.

To further assess the anxiolytic-like effects of eCB augmentation by LM-4131 we analyzed the effects of LM-4131 and the FAAH inhibitor PF-3845 in the light-dark box and the elevated plus-maze. In the light-dark box test we found that PF-3845 (10 mg/kg) and LM-4131 (10 mg/kg) both significantly increased light-zone time ($p < 0.05$ for both drugs) and the number of light-zone entries ($p < 0.001$ PF-3845, and $p < 0.01$ LM-4131) without significantly affecting overall locomotor activity (Fig. 6 a-f). Importantly, the anxiolytic effects of LM-4131 were again blocked by the CB₁ receptor antagonist Rimonabant (3 mg/kg), indicating the behavioral effects were mediated via CB₁ receptor activation (Fig. 6 d-f). In the elevated plus-maze both PF-3845 (10 mg/kg) and LM-4131 (10 mg/kg) significantly reduced open arm latency ($p < 0.01$ for PF-3845 and $p < 0.0001$ for LM-4131; Supplemental Fig. 5), but did not affect other parameters including total distance traveled. Overall, the effects of LM-4131 closely mirror the behavioral profile of PF-3845 in all anxiety measures examined, suggesting that SSCI can exert anxiolytic actions via eCB augmentation in a similar manner to FAAH inhibition. These studies provide proof-of-concept validation that SSCI could represent a novel class of COX-2 based anxiolytic agents that exert anxiolytic actions via eCB activation.

LM-4131 lacks overt cannabimimetic activity *in vivo*

Finally, we examined the relative cannabimimetic effects of LM-4131 *in vivo*. Exogenous activation of CB₁ receptors produces a classical “tetrad” of behavioral effects characterized by hypolocomotion, analgesia, catalepsy and hypothermia⁴¹. Our open field data indicate that LM-4131 does not cause hypolocomotion, and additional studies revealed that LM-4131

did not cause hypothermia, catalepsy, or antinociception in the hot plate test (Fig. 7 a-c). In contrast, the CB₁ agonist Win-55212-2 induced hypothermia, catalepsy and anti-nociception (Fig. 7 a-c). LM-4131 also did not induce memory deficits in the novel object recognition assay when administered prior to object memory retrieval (Fig. 7 d). We also demonstrate that LM-4131 does not cause gastrointestinal hemorrhage, a primary adverse effect of COX-1/2 inhibitors including indomethacin, the parent drug of LM-4131 (Supplemental Fig. 6). Taken together, these data indicate that LM-4131 induces a subset of behavioral effects mediated via eCB activation, but does not cause overt cannabimimetic effects, and also does not cause overt GI toxicity observed with many traditional COX inhibitors including indomethacin.

Discussion

Pharmacological approaches to augment eCB signaling have thus far focused on inhibition of FAAH and MAGL. Both approaches have been validated to robustly augment eCB levels *in vivo*^{17,22}, and exert preclinical therapeutic effects in a variety of pathological conditions. However, both approaches increase non-eCB lipids (NAEs for FAAH inhibition and MAGs for MAGL inhibition) that have biological actions at targets other than cannabinoid receptors⁴². Here we show that COX-2 is a key regulator of eCB levels *in vivo*, and that SSCIs represent a viable alternative approach to augment eCB levels with a high degree of selectivity. In contrast to traditional COX inhibitors, only the SSCI LM-4131 increased AEA without affecting central or peripheral PGs. These data validate the *in vivo* substrate-selectivity of LM-4131 and provide a novel and effective pharmacological strategy to selectively augment central AEA signaling via COX-2 inhibition. Although LM-4131 treatment had an overall significant effect on 2-AG levels, it was quite small and not recapitulated in every experiment, thus any biological significance of this effect remains to be determined. These data suggest that COX-2 preferentially regulates AEA over 2-AG. The larger effects of COX-2 inhibition on AEA over 2-AG may be related to the closer proximity between COX-2 and the site of AEA biosynthesis, and may explain its relative lack of overt cannabimimetic effects³⁷. In support of this notion, FAAH, which is the primary metabolic regulator of AEA, is localized to the same postsynaptic cellular compartment as COX-2⁴³. Furthermore, LM-4131 does not affect levels of non-eCB NAEs or MAGs in the brain or periphery providing enhanced selectivity over FAAH and MAGL inhibition for eCB augmentation. That LM-4131 was able to increase AEA in several peripheral tissues tested suggests that COX-2 plays a widespread role in the regulation of AEA signaling.

Consistent with studies demonstrating that elevating AEA levels via FAAH inhibition exerts anxiolytic-like actions in preclinical models^{22,39,40,44}, we also found that LM-4131 decreased anxiety-like behaviors using multiple validated assays. These data suggest that SSCIs could represent a viable approach to the treatment of mood and anxiety disorders; however, further studies are clearly required to confirm this suggestion. Interestingly, COX-2 inhibition has demonstrated clinical antidepressant efficacy as an adjunct to traditional antidepressants⁴⁵. Our data raise the intriguing possibility that these effects could be in part due to augmentation of brain eCB signaling.

In addition to having beneficial effects in the brain, the substrate-selectivity of LM-4131 could potentially reduce some common side effects mediated by inhibition of PG synthesis by traditional NSAIDs. Gastrointestinal PG production is essential for stimulation of mucosal bicarbonate and mucus secretion as well as increasing mucosal blood flow⁴⁶. As such, traditional NSAIDs are associated with serious gastrointestinal complications. Our data indicate that LM-4131 does not cause overt gastrointestinal hemorrhage as seen with indomethacin. Furthermore, cardiovascular toxicity of COX inhibitors are well-established, and have been suggested to be mediated by inhibition of PG synthesis⁴⁷. As such, SSCI may be devoid of such toxicity since they do not affect PG levels in the heart or lung. Additional research will clearly be required to evaluate the side-effect profile of SSCI relative to traditional COX inhibitors.

Here we have shown that COX-2 is a key regulator of brain eCB signaling *in vivo* and that substrate-selective inhibition of COX-2 could represent anovel pharmacological approach to the treatment of anxiety disorders. Moreover, given the numerous pathological processes in which dysregulation of eCB signaling has been demonstrated, coupled with the high degree of selectivity of SSCIs for eCBs over related non-eCB lipids, we suggest SSCIs could represent a novel class of pharmaceutical agents with broad therapeutic potential.

Online Methods

Materials

Indomethacin was purchased from Sigma Aldrich Chemical (St. Louis, MO). NS-398, SC-560, JZL-184, PF-3845, URB597, PGE₂-d₄, AA-d₈, 2-AG-d₈, and AEA-d₈ were purchased from Cayman Chemical (Ann Arbor, MI). LM-4131 was synthesized as previously described⁴⁸.

In vitro Enzyme Purification and Activity Assays

Wild-type, R120Q, and Y355F COX-2 were expressed in insect cells and purified as described previously⁴⁹. *In vitro* COX-2 inhibition assays were performed as previously described³³. The RAW 264.7 macrophage inhibition assay was performed as previously described⁵⁰. MAGL was purified using BL21(DE3) pLysS E. coli transformed with pET-45b(+) plasmid containing human MGL-His. Cells were grown at 37°C to a density of 0.7 OD and then protein expression induced with IPTG (1 mM). Cells were harvested 4 hr later and proteins purified using Ni-NTA Agarose (Qiagen) as previously described⁵¹. After purification, the protein was dialyzed overnight at 4°C into buffer containing 0 mM HEPES and 0.01% TritonX-100. MAGL inhibition was assessed as previously described⁵¹. Humanized rat FAAH was a generous gift of R. Stevens and B. Cravatt (The Scripps Research Institute). FAAH inhibition was assessed as previously described⁵². Human DAGL α in pcDNA3.1D was expressed in HEK293T cells for 24 hours then harvested and membranes prepared as described previously⁵³. DAGL α activity was assessed using 5 μ g of membrane protein in a 50 μ l reaction of assay buffer containing 50 mM MES (pH 6.5) and 2.5 mM CaCl₂. 1-steroyl-2-arachidonoyl glycerol (SAG) was added directly from a 100% methanol stock for a final concentration of 250 μ M (5% final concentration of methanol in reaction). The reaction was terminated after 15 min by the addition of 200 μ l methanol

containing 125 pmol 2-AG-d₈. The samples were spun down at 2000 ×g and the soluble material injected directly for LC/MS/MS analysis.

Animals

5-7 week old male ICR mice were used for all experiments with the exception of knockout animals (Harlan, Indianapolis, IN). Mice were housed 5 per cage. All behavioral tests were conducted during the light cycle between 0900 and 1700. KO and WT littermate controls for *Faah*^{-/-} and *Ptgs2*^{-/-} mice were derived from heterozygote breeding pairs, bred and genotyped as previously described⁵⁴. *Cnr1*^{-/-} mice were bred from homozygote breeding pairs and genotyped as previously described⁵⁵. All transgenic mice were on an ICR background. Mice were group-housed on a 12:12 light-dark cycle (lights on at 06:00), with food and water available ad libitum. All animal studies were approved by the Vanderbilt Institutional Animal Care and Use Committee and conducted in accordance with the NIH Guide for the Care and Use of Laboratory animals.

Tissue preparation and lipid extraction

Mice were sacrificed by cervical dislocation and decapitation. The brain, lungs, liver, stomach, small intestines, and kidneys were then rapidly removed and frozen on a metal block in dry ice. The tissue was then placed in a tube and stored at -80°C until extraction, usually one day after harvesting. For PG and eCB analysis, lipid extraction from tissue was carried out as described previously⁵⁶.

Open field test

Animals were tested for open-field activity in a novel environment one hour after i.p. injection of compound as previously described²⁰. Briefly, one-hour sessions were performed using automated experimental chambers (27.9 × 27.9 cm; MED-OFA-510; MED Associates, Georgia, VT) under constant illumination within a sound-attenuated room. Analysis of open field activity was performed using Activity Monitor v5.10 (MED Associates).

Light-dark box

Anxiety responses were assessed in a plastic light-dark chamber measuring 20 × 20 cm. Half of the chamber is opaque with a black Plexiglas insert; the other half remains transparent. Photocells recorded the movement of the mice between compartments. Mice were placed individually into the dark compartment at the beginning of the session. Total time spent in the light and dark compartments, the number of light to dark transitions, and total distance travelled during the 20 minute session were measured.

Elevated plus-maze

EPM analysis was conducted using Any Maze tracking software exactly as described previously²⁰.

Rectal temperature, catalepsy, and antinociception

Mice were treated with either LM 4131 (10 mg/kg) or WIN-55,212-2 (10 mg/kg), or corresponding vehicle by IP injection. Every 15 minutes, the rectal temperature of the mice

was taken using a lubricated rectal thermometer for a total of 1 hour post drug injection. To test catalepsy every 15 minutes the hindpaws of the mice were rested on a table and the front paws of the mouse were placed on a metal ring attached to a stand elevated 16 cm above the table. The time for the mouse to place its front paws on the table was recorded. For the hot plate antinociception test, mice were placed on a flat surface that was electrically-heated to 55°C within an open Plexiglas tube, which was cleaned in between testing each mouse with Vimoba, a chlorine dioxide solution. The latency of the mice to respond upon placement on the hot plate apparatus by shaking, hindpaw licking, jumping, or tucking of the forepaws or hindpaws was recorded.

Novel object recognition

Mice were handled 4 days prior to training for at least 1 min per day. During pre-training, mice were placed in an open Plexiglas rectangular chamber for 10 min in order for the mice to become familiar with the testing environment. Twenty-four hours later, the mice were placed into the same rectangular chamber with two identical sample objects, yellow rubber ducks, for 10 min in order for the mice to become familiar with the objects. During training, the sample objects were placed in opposite corners in the back of the chamber 5 cm from each wall and secured by weight to the floor of the chamber. Twenty four hours later, the mice were placed into the chamber again with one sample or familiar object and a novel object, a white leaf statue, for 5 min. During testing, the objects were placed in opposite corners in the back of the chamber 5 cm from each wall and secured by weight to the floor of the chamber. Two hours prior to testing, the mice were treated either with vehicle or the COX-2 inhibitor, LM-4131 (10 mg/kg), by IP injection. To determine exploration time with the sample and novel objects, each mouse was timed when interacting with the sample or novel object when the nose of the mouse was in contact with the object or directed toward the object within a 2 cm distance of the object. The time the mouse spent on top of the objects was not included in the exploration time analyses. In addition, a discrimination ratio (e.g., ratio of a mouse's interaction with a novel object to that mouse's total interaction with both sample and novel objects) was determined. If the discrimination ratio was above 0.5, it was considered that the mouse interacted more with the novel object than with the sample or familiar object.

Mass Spectrometry Analysis

Analytes were quantified using LC-MS/MS on a Quantum triple-quadrupole mass spectrometer in positive-ion mode using selected reaction monitoring. Detection of eicosanoids was performed as previously described⁵⁷. For fatty acid analysis the mobile phases used were 80 µM AgOAc with 0.1% (v/v) acetic acid in H₂O (solvent A) and 120 µM AgOAc with 0.1% (v/v) acetic acid in MeOH (solvent B). The analytes were eluted using a gradient from 20% A to 99% B over 5 minutes. The transitions used were m/z 300→282 for PEA, m/z 328→310 for SEA, m/z 434→416 for OEA, m/z 456→438 for AEA, m/z 464→446 for AEA-d₈, m/z 331→257 for 2-PG, m/z 359→285 for 2-SG, m/z 463→389 for 2-OG, m/z 485→411 for 2-AG, m/z 493→419 for 2-AG-d₈, m/z 519→409 for AA, and m/z 527→417 for AA-d₈. Peak areas for the analytes were normalized to the appropriate internal standard and then normalized to tissue mass for *in vivo* samples.

Statistical Analysis

Statistical analysis was performed using GraphPad Prism® Version 6.0c. For determining statistical significance between groups a two-tailed t-test, one-way ANOVA, or two-way ANOVA with a Sidak's post-test analysis, or multiple t-tests with Holm-Sidak α correction for multiple comparisons was used throughout. F and P values shown correspond to the value obtained from the test used. Large data sets of normalized brain AEA and PG levels ($n > 100$) showed a normal distribution using D'Agostino & Pearson omnibus normality test, 2-AG did not, however visual inspection of the distribution in of 2-AG levels in figure 2f did not show obvious outliers or heavy-tails. No routine analysis of differences in data set variance was conducted therefore t-tests did not assume equal variances (Welch correction). Error bars represent S.E.M. throughout. No treatment blinding was conducted. Sample sized were based on previous studies⁵⁶. N for each group represents number of mice, i.e. independent biological replicate. Mice were arbitrarily assigned to treatment group in a manner that resulted in approximately equal sample sized per treatment group. Each treatment group was represented at least once per cage of mice. No mice were excluded from the statistical analysis.

Supplementary Material

Refer to Web version on PubMed Central for supplementary material.

Acknowledgments

These studies were supported by NIH grants MH090412 (S.P.), CA89450, GM15431, NS064278 (L.J.M), DA031572 (D.J.H), HL96967, HL109199 (J.R.), MH063232, NS078291 (R.J.C), T32-MH065215 (B.C.S), and the A.B. Hancock Jr. Memorial Laboratory for Cancer Research. Analytical studies were conducted in the Vanderbilt University Mass Spectrometry Core facility and all behavioral experiments were conducted in the Vanderbilt University Medical Center Mouse Neurobehavioral Core facility. We thank K. Masuda, M. Brown, R. Stevens, and B. Cravatt for FAAH knockout mice. The content of this article is solely the responsibility of the authors and does not necessarily represent the official views of the US National Institutes of Health.

References

1. Di Marzo V. Endocannabinoids: synthesis and degradation. Reviews of physiology, biochemistry and pharmacology. 2008; 160:1–24.
2. Piomelli D. The molecular logic of endocannabinoid signalling. Nature reviews. 2003; 4:873–884.
3. Ahn K, McKinney MK, Cravatt BF. Enzymatic pathways that regulate endocannabinoid signaling in the nervous system. Chem Rev. 2008; 108:1687–1707. [PubMed: 18429637]
4. Kunos G. Understanding metabolic homeostasis and imbalance: what is the role of the endocannabinoid system? The American journal of medicine. 2007; 120:S18–24. discussion S24. [PubMed: 17720356]
5. Di Marzo V, Piscitelli F, Mechoulam R. Cannabinoids and endocannabinoids in metabolic disorders with focus on diabetes. Handbook of experimental pharmacology. 2011:75–104. [PubMed: 21484568]
6. Guindon J, Hohmann AG. The endocannabinoid system and pain. CNS & neurological disorders drug targets. 2009; 8:403–421. [PubMed: 19839937]
7. Hohmann AG, Suplita RL 2nd. Endocannabinoid mechanisms of pain modulation. The AAPS journal. 2006; 8:E693–708. [PubMed: 17233533]
8. Lichtman AH, Varvel SA, Martin BR. Endocannabinoids in cognition and dependence. Prostaglandins, leukotrienes, and essential fatty acids. 2002; 66:269–285.

9. Patel S, Hillard CJ. Adaptations in endocannabinoid signaling in response to repeated homotypic stress: a novel mechanism for stress habituation. *Eur J Neurosci*. 2008; 27:2821–2829. [PubMed: 18588527]
10. Lutz B. Endocannabinoid signals in the control of emotion. *Curr Opin Pharmacol*. 2009; 9:46–52. [PubMed: 19157983]
11. Centonze D, Finazzi-Agro A, Bernardi G, Maccarrone M. The endocannabinoid system in targeting inflammatory neurodegenerative diseases. *Trends in pharmacological sciences*. 2007; 28:180–187. [PubMed: 17350694]
12. Bisogno T, Di Marzo V. Cannabinoid receptors and endocannabinoids: role in neuroinflammatory and neurodegenerative disorders. *CNS & neurological disorders drug targets*. 2010; 9:564–573. [PubMed: 20632970]
13. Bifulco M, Laezza C, Gazerro P, Pentimalli F. Endocannabinoids as emerging suppressors of angiogenesis and tumor invasion (review). *Oncology reports*. 2007; 17:813–816. [PubMed: 17342320]
14. Lopez-Rodriguez ML, Viso A, Ortega-Gutierrez S, Diaz-Laviada I. Involvement of cannabinoids in cellular proliferation. *Mini reviews in medicinal chemistry*. 2005; 5:97–106. [PubMed: 15638794]
15. Tam J, et al. Involvement of neuronal cannabinoid receptor CB1 in regulation of bone mass and bone remodeling. *Molecular pharmacology*. 2006; 70:786–792. [PubMed: 16772520]
16. Cravatt BF, et al. Molecular characterization of an enzyme that degrades neuromodulatory fatty-acid amides. *Nature*. 1996; 384:83–87. [PubMed: 8900284]
17. Long JZ, et al. Selective blockade of 2-arachidonoylglycerol hydrolysis produces cannabinoid behavioral effects. *Nat Chem Biol*. 2009; 5:37–44. [PubMed: 19029917]
18. Mangieri RA, Piomelli D. Enhancement of endocannabinoid signaling and the pharmacotherapy of depression. *Pharmacological research: the official journal of the Italian Pharmacological Society*. 2007; 56:360–366.
19. Sciolino NR, Zhou W, Hohmann AG. Enhancement of endocannabinoid signaling with JZL184, an inhibitor of the 2-arachidonoylglycerol hydrolyzing enzyme monoacylglycerol lipase, produces anxiolytic effects under conditions of high environmental aversiveness in rats. *Pharmacological research: the official journal of the Italian Pharmacological Society*. 2011
20. Sumislawski JJ, Ramikie TS, Patel S. Reversible gating of endocannabinoid plasticity in the amygdala by chronic stress: a potential role for monoacylglycerol lipase inhibition in the prevention of stress-induced behavioral adaptation. *Neuropsychopharmacology*. 2011; 36:2750–2761. [PubMed: 21849983]
21. Naidu PS, et al. Evaluation of fatty acid amide hydrolase inhibition in murine models of emotionality. *Psychopharmacology*. 2007; 192:61–70. [PubMed: 17279376]
22. Kathuria S, et al. Modulation of anxiety through blockade of anandamide hydrolysis. *Nature medicine*. 2003; 9:76–81.
23. Gaetani S, et al. The endocannabinoid system as a target for novel anxiolytic and antidepressant drugs. *International review of neurobiology*. 2009; 85:57–72. [PubMed: 19607961]
24. Makriyannis A, Mechoulam R, Piomelli D. Therapeutic opportunities through modulation of the endocannabinoid system. *Neuropharmacology*. 2005; 48:1068–1071. [PubMed: 15885714]
25. Di Marzo V. The endocannabinoid system: its general strategy of action, tools for its pharmacological manipulation and potential therapeutic exploitation. *Pharmacological research: the official journal of the Italian Pharmacological Society*. 2009; 60:77–84.
26. Piomelli D. The endocannabinoid system: a drug discovery perspective. *Curr Opin Investig Drugs*. 2005; 6:672–679.
27. Kozak KR, Rowlinson SW, Marnett LJ. Oxygenation of the endocannabinoid, 2-arachidonoylglycerol, to glyceryl prostaglandins by cyclooxygenase-2. *J Biol Chem*. 2000; 275:33744–33749. [PubMed: 10931854]
28. Rouzer CA, Marnett LJ. Non-redundant functions of cyclooxygenases: oxygenation of endocannabinoids. *J Biol Chem*. 2008; 283:8065–8069. [PubMed: 18250160]
29. Kim J, Alger BE. Inhibition of cyclooxygenase-2 potentiates retrograde endocannabinoid effects in hippocampus. *Nature neuroscience*. 2004; 7:697–698. [PubMed: 15184902]

30. Glaser ST, Kaczocha M. Cyclooxygenase-2 mediates anandamide metabolism in the mouse brain. *J Pharmacol Exp Ther.* 2010; 335:380–388. [PubMed: 20702753]
31. Staniaszek LE, Norris LM, Kendall DA, Barrett DA, Chapman V. Effects of COX-2 inhibition on spinal nociception: the role of endocannabinoids. *Br J Pharmacol.* 2010; 160:669–676. [PubMed: 20590570]
32. Bishay P, et al. R-flurbiprofen reduces neuropathic pain in rodents by restoring endogenous cannabinoids. *PLoS One.* 2010; 5:e10628. [PubMed: 20498712]
33. Duggan KC, et al. (R)-Profens are substrate-selective inhibitors of endocannabinoid oxygenation by COX-2. *Nat Chem Biol.* 2011; 7:803–809. [PubMed: 22053353]
34. Prusakiewicz JJ, Duggan KC, Rouzer CA, Marnett LJ. Differential sensitivity and mechanism of inhibition of COX-2 oxygenation of arachidonic acid and 2-arachidonoylglycerol by ibuprofen and mefenamic acid. *Biochemistry.* 2009; 48:7353–7355. [PubMed: 19603831]
35. Knihinicki RD, Day RO, Graham GG, Williams KM. Stereoselective disposition of ibuprofen and flurbiprofen in rats. *Chirality.* 1990; 2:134–140. [PubMed: 2252842]
36. Kalgutkar AS, et al. Biochemically based design of cyclooxygenase-2 (COX-2) inhibitors: facile conversion of nonsteroidal antiinflammatory drugs to potent and highly selective COX-2 inhibitors. *Proceedings of the National Academy of Sciences of the United States of America.* 2000; 97:925–930. [PubMed: 10639181]
37. Long JZ, et al. Dual blockade of FAAH and MAGL identifies behavioral processes regulated by endocannabinoid crosstalk in vivo. *Proc Natl Acad Sci U S A.* 2009; 106:20270–20275. [PubMed: 19918051]
38. Kinsey SG, O'Neal ST, Long JZ, Cravatt BF, Lichtman AH. Inhibition of endocannabinoid catabolic enzymes elicits anxiolytic-like effects in the marble burying assay. *Pharmacol Biochem Behav.* 2010; 98:21–27. [PubMed: 21145341]
39. Rossi S, et al. Preservation of striatal cannabinoid CB1 receptor function correlates with the antianxiety effects of fatty acid amide hydrolase inhibition. *Molecular pharmacology.* 2010; 78:260–268. [PubMed: 20424126]
40. Moreira FA, Kaiser N, Monory K, Lutz B. Reduced anxiety-like behaviour induced by genetic and pharmacological inhibition of the endocannabinoid-degrading enzyme fatty acid amide hydrolase (FAAH) is mediated by CB1 receptors. *Neuropharmacology.* 2008; 54:141–150. [PubMed: 17709120]
41. Fride E, Perchuk A, Hall FS, Uhl GR, Onaivi ES. Behavioral methods in cannabinoid research. *Methods in molecular medicine.* 2006; 123:269–290. [PubMed: 16506414]
42. O'Sullivan SE. Cannabinoids go nuclear: evidence for activation of peroxisome proliferator-activated receptors. *Br J Pharmacol.* 2007; 152:576–582. [PubMed: 17704824]
43. Cristino L, et al. Immunohistochemical localization of anabolic and catabolic enzymes for anandamide and other putative endovanilloids in the hippocampus and cerebellar cortex of the mouse brain. *Neuroscience.* 2008; 151:955–968. [PubMed: 18248904]
44. Patel S, Hillard CJ. Pharmacological evaluation of cannabinoid receptor ligands in a mouse model of anxiety: further evidence for an anxiolytic role for endogenous cannabinoid signaling. *J Pharmacol Exp Ther.* 2006; 318:304–311. [PubMed: 16569753]
45. Muller N, Schwarz MJ. COX-2 inhibition in schizophrenia and major depression. *Curr Pharm Des.* 2008; 14:1452–1465. [PubMed: 18537668]
46. Patrignani P, Tacconelli S, Bruno A, Sostres C, Lanos A. Managing the adverse effects of nonsteroidal anti-inflammatory drugs. *Expert review of clinical pharmacology.* 2011; 4:605–621. [PubMed: 22114888]
47. Yu Y, et al. Vascular COX-2 modulates blood pressure and thrombosis in mice. *Science translational medicine.* 2012; 4:132ra154.
48. Kalgutkar AS, Marnett AB, Crews BC, Rimmel RP, Marnett LJ. Ester and amide derivatives of the nonsteroidal antiinflammatory drug, indomethacin, as selective cyclooxygenase-2 inhibitors. *J Med Chem.* 2000; 43:2860–2870. [PubMed: 10956194]
49. Rowlinson SW, Crews BC, Lanzo CA, Marnett LJ. The binding of arachidonic acid in the cyclooxygenase active site of mouse prostaglandin endoperoxide synthase-2 (COX-2) - A putative

- L-shaped binding conformation utilizing the top channel region. *J Biol Chem.* 1999; 274:23305–23310. [PubMed: 10438506]
50. Rouzer CA, Marnett LJ. Glyceryl prostaglandin synthesis in lipopolysaccharide-treated RAW264.7 cells is augmented by interferon-gamma and granulocytemacrophage colony stimulating factor. *Prostag Oth Lipid M.* 2006; 79:146–147.
51. Blankman JL, Simon GM, Cravatt BF. A comprehensive profile of brain enzymes that hydrolyze the endocannabinoid 2-arachidonoylglycerol. *Chem Biol.* 2007; 14:1347–1356. [PubMed: 18096503]
52. Ahn K, et al. Discovery and Characterization of a Highly Selective FAAH Inhibitor that Reduces Inflammatory Pain. *Chem Biol.* 2009; 16:411–420. [PubMed: 19389627]
53. Pedicord DL, et al. Molecular characterization and identification of surrogate substrates for diacylglycerol lipase alpha. *Biochem Bioph Res Co.* 2011; 411:809–814.
54. Uddin MJ, et al. Fluorinated COX-2 Inhibitors as Agents in PET Imaging of Inflammation and Cancer. *Cancer Prev Res.* 2011; 4:1536–1545.
55. Pan B, Hillard CJ, Liu QS. D-2 Dopamine Receptor Activation Facilitates Endocannabinoid-Mediated Long-Term Synaptic Depression of GABAergic Synaptic Transmission in Midbrain Dopamine Neurons via cAMP-Protein Kinase A Signaling. *J Neurosci.* 2008; 28:14018–14030. [PubMed: 19109485]
56. Patel S, Kingsley PJ, Mackie K, Marnett LJ, Winder DG. Repeated Homotypic Stress Elevates 2-Arachidonoylglycerol Levels and Enhances Short-Term Endocannabinoid Signaling at Inhibitory Synapses in Basolateral Amygdala. *Neuropsychopharmacol.* 2009; 34:2699–2709.
57. Kingsley PJ, Marnett LJ. LC-MS-MS analysis of neutral eicosanoids. *Method Enzymol.* 2007; 433:91–+.

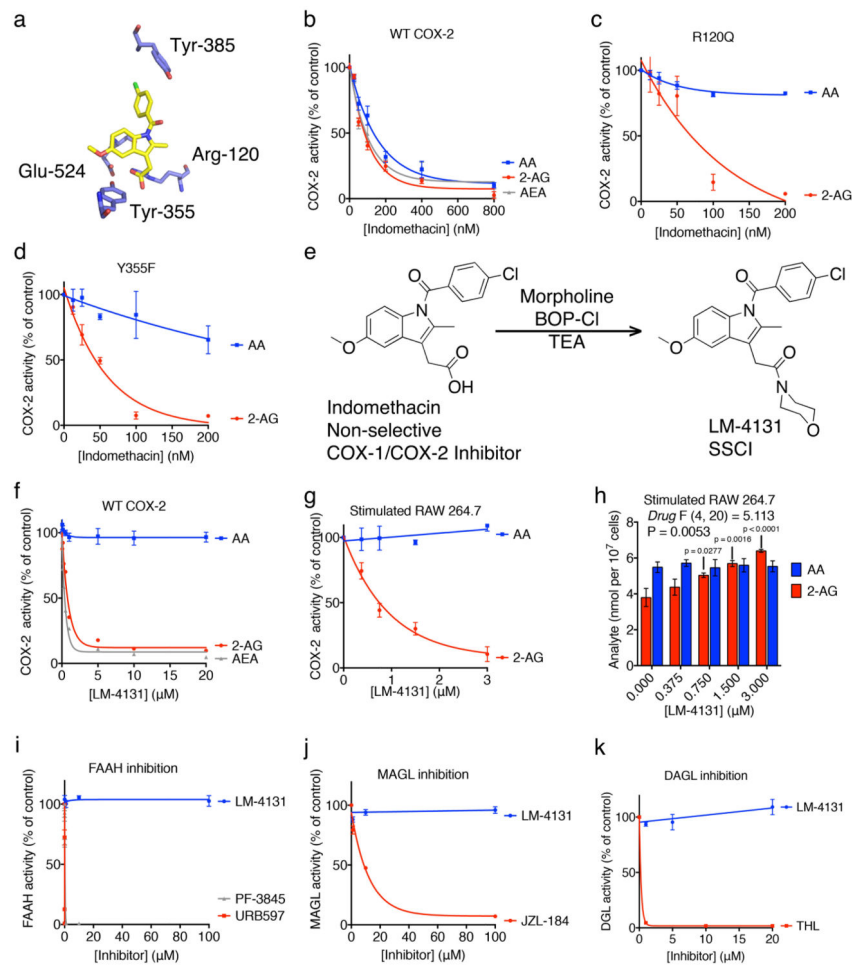


Figure 1. Molecular determinants of substrate-selective pharmacology

(a) The crystal structure of indomethacin bound to mCOX-2 highlighting the interactions between the inhibitor and Arg-120 and Tyr-355 of the COX-2 active site. (b) Indomethacin inhibition of AA (blue), 2-AG (red), and AEA (grey) oxygenation by WT mCOX-2. (c) Indomethacin inhibition of 2-AG (red) but not AA (blue) oxygenation by R120Q COX-2. (d) Indomethacin inhibition of 2-AG (red) but not AA (blue) oxygenation by Y355F COX-2. (e) Conversion of indomethacin to LM-4131, an SSIC. (f) LM-4131 inhibition of AEA (grey) and 2-AG (red), but not AA (blue), oxygenation by WT mCOX-2. (g) Inhibition of 2-AG (red), but not AA (blue), oxygenation by COX-2 in stimulated RAW 264.7 macrophages by LM-4131. (h) Levels of 2-AG (red) and AA (blue) in stimulated RAW 264.7 macrophages in response to increasing concentrations of LM-4131. LM-4131 significantly increased 2-AG levels at 0.75 μ M, 1.5 μ M, and 3 μ M. Data shown are mean \pm S.E.M with $n = 3$ cell plates for each point. Significance determined using a two-way ANOVA followed by Holm-Sidak's multiple comparisons post-test. (i) Effects of LM-4131, PF-3845, and URB597 on FAAH activity. (j) Effects of LM-4131 and JZL-184 on MAGL activity. (k) Effects of LM-4131 and THL on DAGL activity.

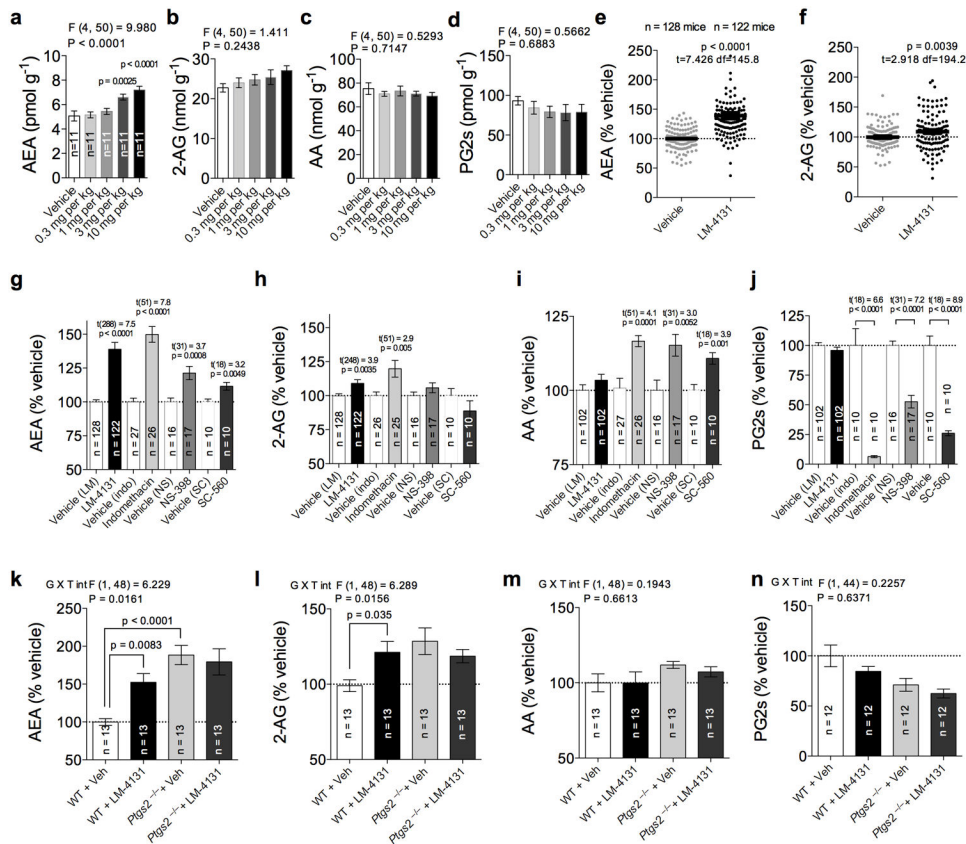


Figure 2. LM-4131 is an *in vivo* bioactive SSCI

(a-d) Effects of increasing doses of LM-4131 on AEA, 2-AG, AA and PG in brain 2 hours after i.p. injection. (e-f) Combined data from multiple cohorts of mice showing average magnitude of LM-4131 effects on brain AEA and 2-AG levels as % vehicle treatment. (g-j) Effects of LM-4131, indomethacin, NS-398, and SC-560 on brain (g) AEA, (h) 2-AG, (i) AA, and (j) PG levels as a % of corresponding vehicle group. (k-n) Effects of LM-4131 on brain (k) AEA, (l) 2-AG, (m) AA, and (n) PG in WT and *Ptg2s*^{-/-} mice. F and P values shown for one-way ANOVA, and p values for Dunnett's post hoc analysis show in (a-d); t-statistics and p values shown for unpaired two-tailed t-tests in (e-f and g-j; drug treatment vs. corresponding vehicle group); F and P values for genotype × LM-treatment interaction (G × T int) by two-way ANOVA, and p values for Sidak's multiple comparisons post hoc test shown in figures (k-l). n=number of mice per treatment group indicated in bars. Error bars represent S.E.M.

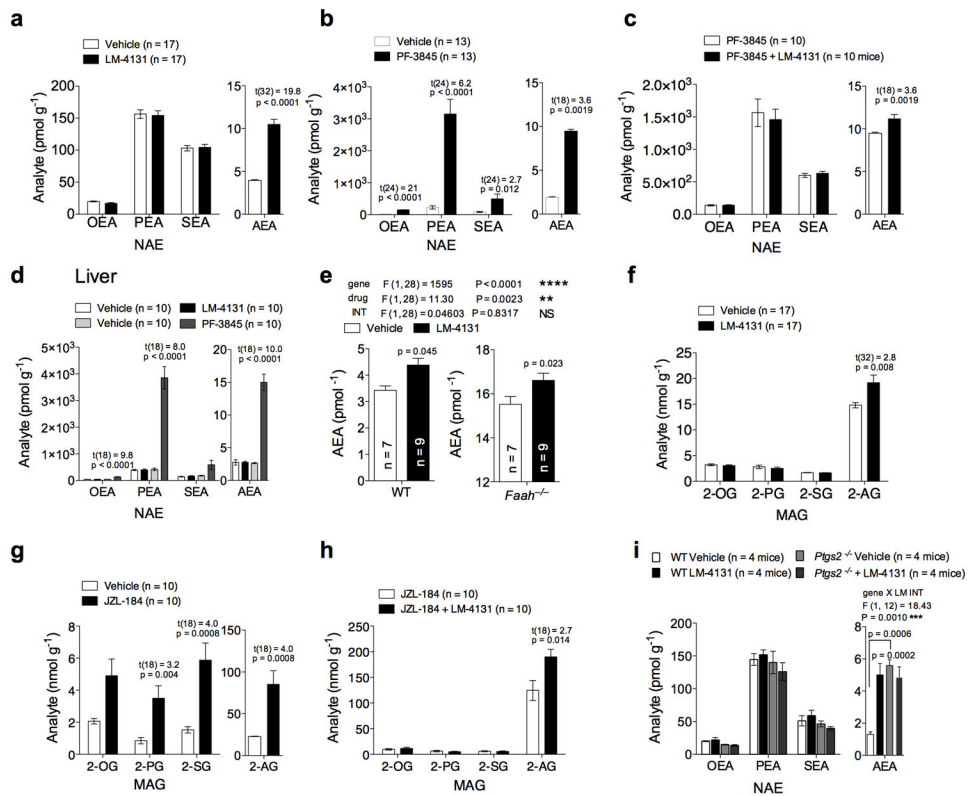


Figure 3. LM-4131 selectively increases brain eCBs without affecting related lipids
 Effects of (a) LM-4131 and (b) PF-3845 on brain NAE levels two hours after i.p. injection. (c) Effect of PF-3845 alone, or in combination with LM-4131, on brain NAE levels. (d) Effects of LM-4131 and PF-3845 on liver NAE levels. (e) Effects of LM-4131 on brain AEA levels in WT and *Faah*^{-/-} mice. Effects of (f) LM-4131 and (g) JZL-184 on brain MAG levels. (h) Effects of JZL-184 alone or in combination with LM-4131 on brain MAG levels. (i) Effects of LM-4131 on brain NAEs in WT and *Ptgs2*^{-/-} mice. Multiplicity corrected P values and t-statistics by unpaired two-tailed t-tests with Holm-Sidak multiple comparisons α correction are shown in (a-d and f-h); F and P values for main effects of two-way ANOVA followed, and p values for Sidak's post hoc multiple comparisons test shown in (e); F and P values for genotype \times LM treatment interaction by two-way ANOVA, and p values for Sidak's multiple comparisons post hoc test for AEA levels shown in (i). n = number of mice per treatment group indicated in bars. Error bars represent S.E.M.

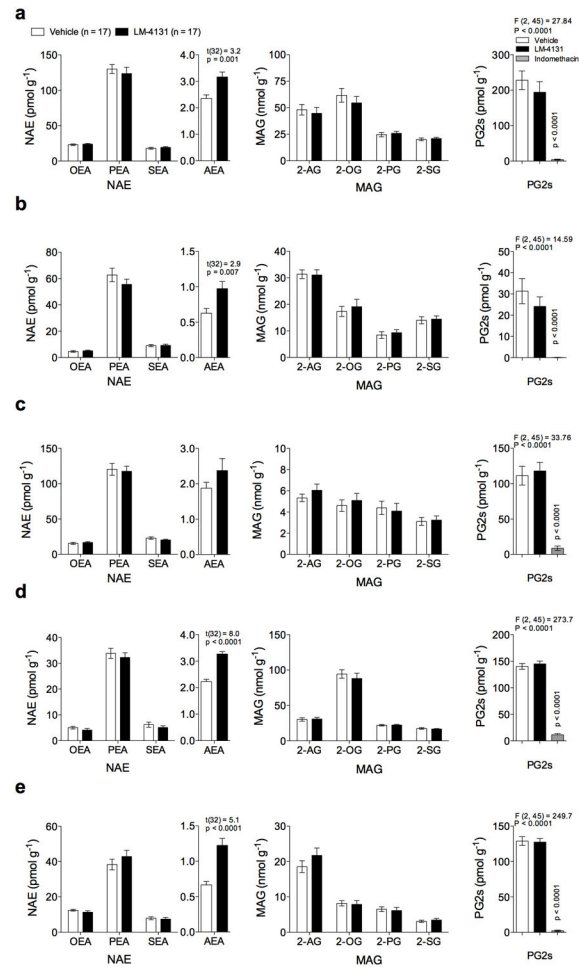


Figure 4. LM-4131 selectively increases AEA in peripheral tissues

Effects of LM-4131 on NAE, MAG, and PG levels in the (a) stomach, (b) small intestine, (c) heart, (d) kidney, and (e) lung two hours after injection. For comparison, the effects of indomethacin on PG levels are shown for each tissue. Multiplicity corrected p values and t-statistics by unpaired two-tailed t-tests with Holm-Sidak multiple comparisons α correction given in (a-e); F and P values for one-way ANOVA, followed by p values from Dunnett's post hoc analysis given for PG analyses in (a-e). n=number of mice per treatment group indicated. Error bars represent S.E.M.

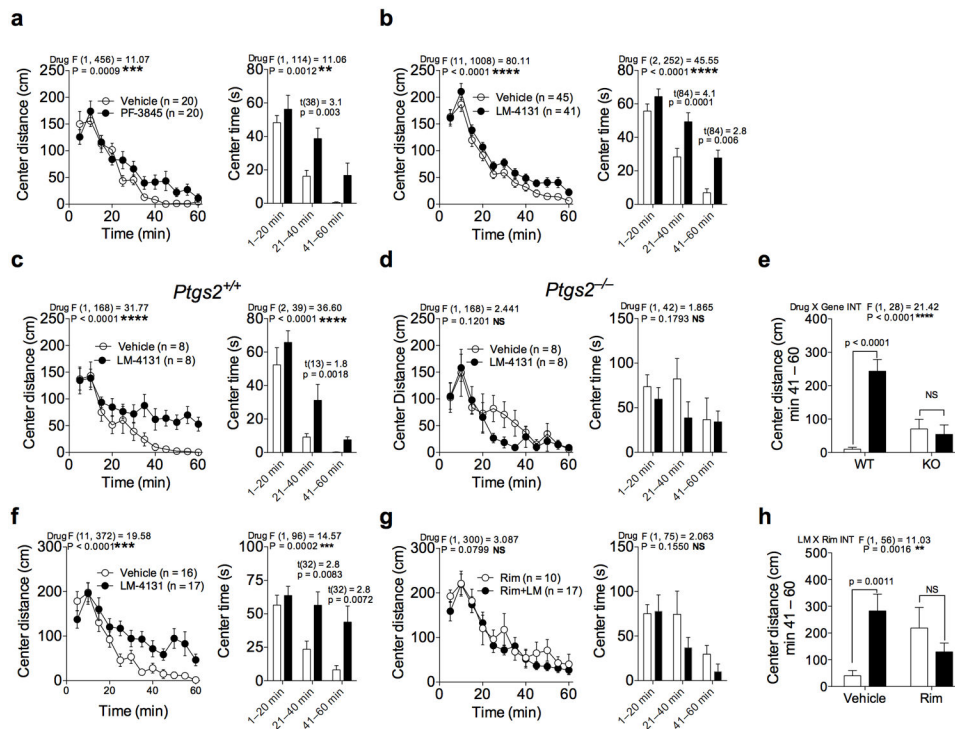


Figure 5. LM-4131 reduces anxiety-like behaviors in the novel open field

Effects of (a) PF-3845 and (b) LM-4131 on center distance and center time traveled in the open field over time. (c-e) Effects of LM-4131 on center distance and center time in the open field in WT and *Ptgs2*^{-/-} mice. (e) Summary data for LM-4131 effects in WT and *Ptgs2*^{-/-} mice on total center distance during the last 20 minutes of the assay. (f-h) Effects of LM-4131 in (f) vehicle or (g) Rimonabant (Rim) pretreated mice. (h) Summary data for LM-4131 effects after vehicle or Rim pretreatment on total center distance during the last 20 minutes of the assay. F and P values for drug effects by two-way repeated measures ANOVA given for (a-d and f-g); multiplicity corrected p values and t-statistics by unpaired two-tailed t-tests with Holm-Sidak multiple comparisons α correction given for center time figures for each significant time epoch in (a-d and f-g); F and P values for genotype \times LM or LM \times Rim pretreatment interaction given for (e) and (h), respectively. Multiplicity corrected P values by Sidak's multiple comparisons post hoc test after ANOVA as indicated in (e and h). n = number of mice per treatment group. Error bars represent S.E.M.

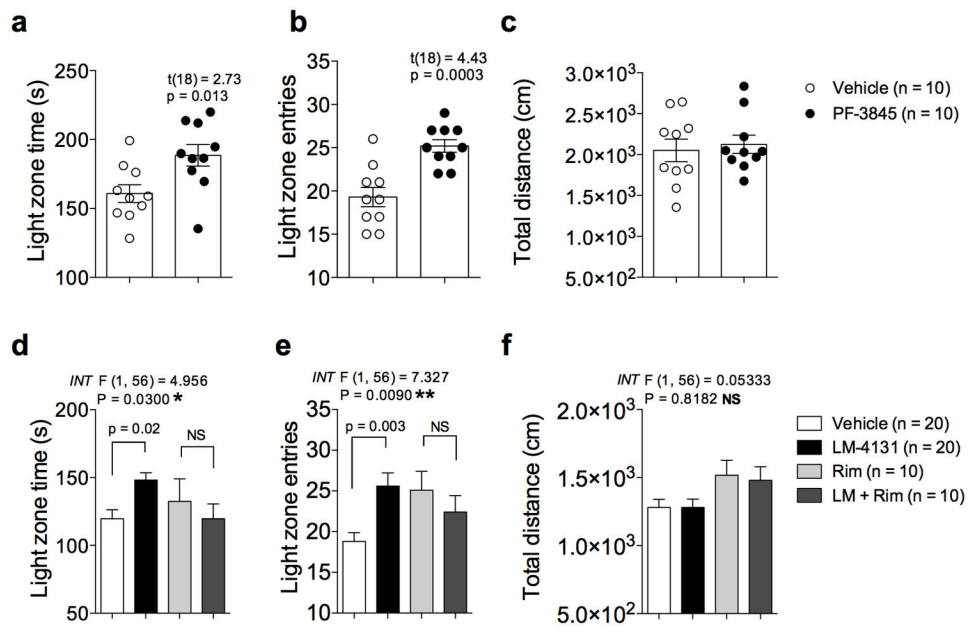


Figure 6. LM-4131 reduces anxiety behaviors in the light-dark box

(a-c) Effects of PF-3845 on (a) light zone time, (b) light zone entries, and (c) total distance travelled in the light-dark box assay. (d-f) Effects of LM-4131 with or without Rim pretreatment on parameters of the light-dark box assay. P values and t-statistics by unpaired two-tailed t-tests given (a-c); F and P values for LM × Rim pretreatment interaction (INT) by two-way ANOVA shown in (d-f); multiplicity corrected P values by Sidak's multiple comparisons post hoc test after ANOVA indicated in (d-f). n=number of mice per treatment group indicated in figure. Error bars represent S.E.M.

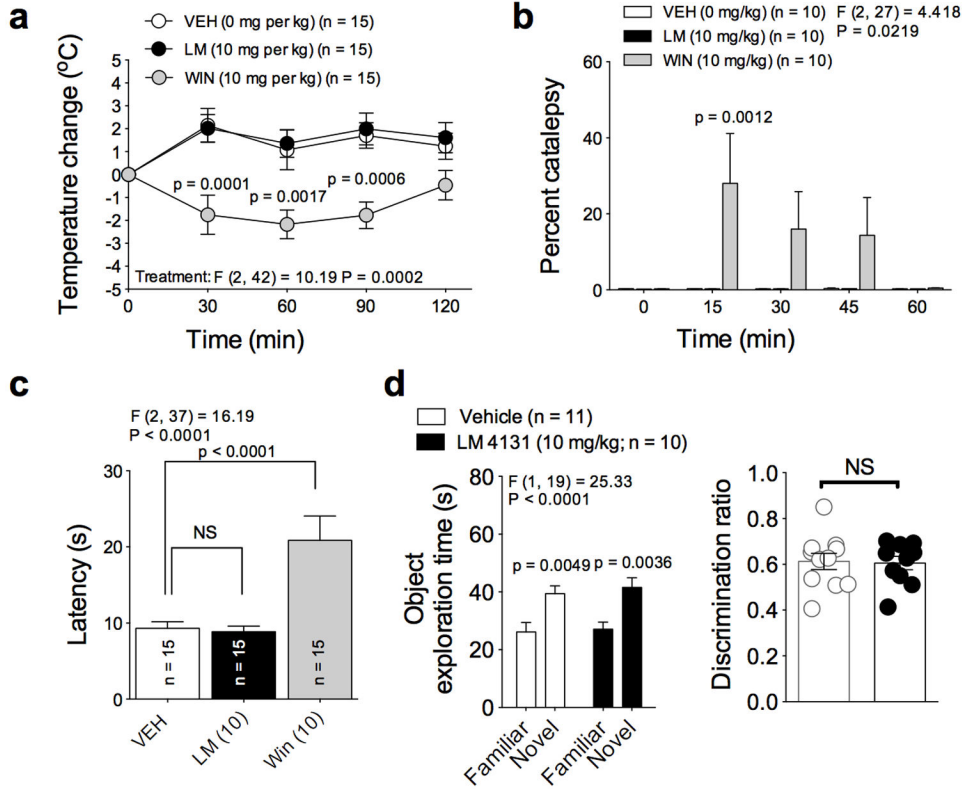


Figure 7. LM-4131 does not exert overt cannabimimetic effects *in vivo*
 (a) Effects of vehicle, LM-4131, and Win 55212-2 on rectal temperature over time. (b) Effects of vehicle, LM-4131, and Win 55212-2 on catalepsy over time. (c) Effects of vehicle, LM-4131, and Win 55212-2 on antinociception in the hot plate test. (d) Effects of LM-4131 on novel object recognition. F and P values for drug treatment effects by two-way ANOVA shown for (a-b), and for novelty recognition factor by two-way ANOVA in (d); F and P values for drug effect by one-way ANOVA shown for (c). Multiplicity corrected P values by Sidak's multiple comparisons post hoc test (a-b, and d) and by Dunnett's post hoc test (c) are shown. n =number of mice per treatment group indicated in figure. Error bars represent S.E.M.